TRAFFIC STATE ESTIMATION FROM PARTIAL BLUETOOTH AND VOLUME OBSERVATIONS: CASE STUDY IN THE BRISBANE METROPOLITAN AREA

A. NANTES [a*], D. NGODUY [b], M. MISKA [a] and E. CHUNG [a]
[a] *Department of Civil Engineering, Queensland University of Technology, Australia*
**Email: a.nantes@qut.edu.au*
[b] *Institute for Transport Studies, The University of Leeds, Leeds, U.K.*

ABSTRACT

The application of the Bluetooth (BT) technology to transportation has been enabling researchers to make accurate travel time observations, in freeway and arterial roads. The Bluetooth traffic data are generally incomplete, for they only relate to those vehicles that are equipped with Bluetooth devices, and that are detected by the Bluetooth sensors of the road network. The fraction of detected vehicles versus the total number of transiting vehicles is often referred to as Bluetooth Penetration Rate (BTPR). The aim of this study is to precisely define the spatio-temporal relationship between the quantities that become available through the partial, noisy BT observations; and the hidden variables that describe the actual dynamics of vehicular traffic. To do so, we propose to incorporate a multi-class traffic model into a Sequential Montecarlo Estimation algorithm. Our framework has been applied for the empirical travel time investigations into the Brisbane Metropolitan region.

Keywords: arterial traffic; traffic state estimation; Bluetooth data; particle filter

1. BACKGROUND

Recent rapid advances in information technology have led to various data collection systems which enrich the sources of empirical data for the traffic state estimation problems. In practice, traffic data are collected from loop detectors, floating cars, cell-phones, video cameras, remote sensing, etc. Particularly, the application of the Bluetooth (BT) technology to transportation has been enabling researchers to make accurate travel time observations, in freeway and arterial roads. Much literature has been published on the estimation and prediction of traffic state from aggregate, partial data, through Bayesian filters (Y. et al. 2012; Work et al. 2009; Mihaylova, Boel and Hegyi 2007) and data fusion techniques (Bachmann et al. 2013; Mehran and Kuwahara 2013). However, very little of it appears to deal with the simultaneous reconstruction of the interrupted arterial traffic state, from BT and stop line detectors, and the state of the BT traffic itself. Traffic states describe the traffic situation – such as free-flow, congestion, stop-and-go, synchronized and oscillatory phenomena – in space and time, in terms of parameters, such as density, flow, and speed. Understanding the dynamical relationships between the state of BT vehicles and the overall traffic state may enable the estimation and prediction of various complex urban traffic situations, by only using a limited set of BT observations.

The Bluetooth traffic data are generally incomplete, for they only relate to those vehicles that are equipped with Bluetooth devices, and that are detected by the Bluetooth sensors of the road network. Some vehicles may not be BT-enabled, and some of the BT-enabled vehicles may be missed by the BT sensors. The fraction of detected vehicles versus the total number of transiting vehicles is often referred to as Bluetooth Penetration Rate (BTPR). Not only is the BTPR unknown, but is also a function of time and space. Nevertheless, the detected vehicles will still flow according to the same macroscopic laws that describe the flow of all vehicles, observable and non-observable. The aim of this study is thus to precisely define the spatio-temporal relationship between the quantities that become available through the partial, noisy BT observations and the hidden variables that describe the actual dynamics of vehicular traffic. In this work, we propose to study the traffic dynamics through a

two-class continuum model. Specifically, we assign the BT-equipped vehicles to one class (*BT class*) and the entire population of vehicles to the other class (*mixed-class*). We will incorporate our model into a Sequential Montecarlo Estimation (SME) algorithm, in order to unveil the current and future distributions of total flow and BTPRs. This is a so-called model based traffic state estimator, which is an optimization problem of combining model predictions from a traffic model and traffic measurements from sensors. Our framework will be tested in the Brisbane Metropolitan region.

This paper makes the following contributions:
1. introduces a Cell Transmission Model (CTM)-based description of the dynamics of the Bluetooth vehicles
2. introduces a model for the macroscopic description of signalised intersections
3. introduces a framework for the simultaneous, on-line estimation of the traffic state, for the mixed class and Bluetooth class

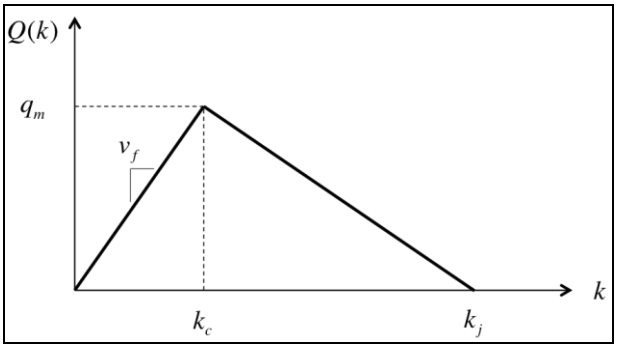

Figure 1. Triangular Fundamental Diagram

2. TWO-CLASS FORMULATION OF ARTERIAL TRAFFIC

In order to estimate the complete state of a system, through an observer-based estimator, a complete model of the system is needed. In this paper, the dynamics of the arterial traffic is described through a single-pipe *two-class* kinematic wave model. The two classes selected are the vehicles detectable by the Bluetooth scanners; and the *mixed class*, of all vehicles, whose volumes at the intersections are typically available through stop-line detectors. As we shall see, the model proposed will enable the estimation of the traffic state upon incomplete and noisy Bluetooth and volume observations. Our system is based on the LWR model (Lighthill and Whitham 1955; Richards 1956), involving a partial differential equation for the conservation of vehicles within the target road section, of the form:

$$\frac{\partial k_u}{\partial t} + \frac{\partial}{\partial x} q_u(k_u) = 0 \qquad (1)$$

where k_u and q_u are the density and flow, respectively, of the generic class u, for example, the *Bluetooth* or the *mixed* class. Henceforth, the subscript u will be used to indicate both the Bluetooth-class and the mixed class; b will denote the Bluetooth class only; no subscript will be used for the variables of the mixed class. Eq. (1) is often discretized using the Godunov scheme, known as Cell-Transmission-Model (CTM), introduced by Daganzo (1994, 1995):

$$k_{u,i}^{t+1} = k_{u,i}^{t} + \frac{\Delta t_{\text{sim}}}{\Delta x_i}\left(q_{u,i}^{\text{in},t} - q_{u,i}^{\text{out},t}\right) \qquad (2)$$

According to this scheme, the road is partitioned into cells. The length of the i-th cell is denoted by Δx_i. Time is partitioned into (simulation) time steps of equal length, Δt_{sim}. The density of the vehicles

of class u, within the i-th cell, at time t, is denoted by $k_{u,i}^{t}$. Finally, $q_{u,i}^{\text{in},t}$ and $q_{u,i}^{\text{out},t}$ are the flow of the class u, into and from cell i, respectively, at time t. The mixed class flow of the section is computed as the minimum between the demand from the upstream cell, and the supply of the current cell. More formally we have

$$\begin{cases} \delta_i^t = Q_i[\min(k_i^t, k_{c,i})] \\ \sigma_i^t = Q_i[\max(k_i^t, k_{c,i})] \\ q_i^{\text{in},t} = \min(\delta_{i-1}^t, \sigma_i^t) \\ q_i^{\text{out},t} = \min(\delta_i^t, \sigma_{i+1}^t) \end{cases} \tag{3}$$

where Q_i is the flow-density fundamental relation for cell i (see Figure 1 as an example); δ_i^t and σ_i^t are the demand and supply, respectively, for cell i, at time t. Finally, $k_{c,i}$ is the *critical density* of cell i. Since the Bluetooth vehicles represent a fraction, λ, of the entire flow we can write

$$\delta_{b,i}^t = \lambda_i^t \delta_i^t \qquad \text{and} \qquad \sigma_{b,i}^t = \lambda_{i-1}^t \sigma_i^t \tag{4}$$

with $\delta_{b,i}^t$ and $\sigma_{b,i}^t$ being the demand and supply, respectively, for the Bluetooth class. Finally, λ_i^t denotes the Bluetooth Penetration Rate (BTPR); this is the proportion of Bluetooth vehicles found in cell i, at time t. This parameter can be determined as follows:

$$\lambda_i^t = \begin{cases} \dfrac{k_{b,i}^t}{k_i^t} & \text{if } k_i^t \neq 0 \\ 0 & \text{otherwise} \end{cases} \tag{5}$$

here $k_{b,i}^t$ is the density of the Bluetooth class in cell i, at time t. For each cell, the Bluetooth-specific density is determined similarly to the density in the minimum supply-demand method presented earlier, that is:

$$k_{b,i}^{t+1} = k_{b,i}^t + \frac{\Delta t_{\text{sim}}}{\Delta x_i}(q_{b,i}^{\text{in},t} - q_{b,i}^{\text{out},t}) \tag{6}$$

$$\text{with} \quad q_{b,i}^{\text{in},t} = \min(\delta_{b,i-1}^t, \sigma_{b,i}^t) \quad \text{and} \quad q_{b,i}^{\text{out},t} = \min(\delta_{b,i}^t, \sigma_{b,i+1}^t)$$

It is reasonable to assume that the mixed class and the Bluetooth class both move at the same average speed, $v_{u,i}^t$, for any cell i, at any time t. This speed reads

$$v_{u,i}^t = \frac{Q_i(k_i^t)}{k_i^t} \tag{7}$$

2.1 Multi-Class Merge and Diverge Rules

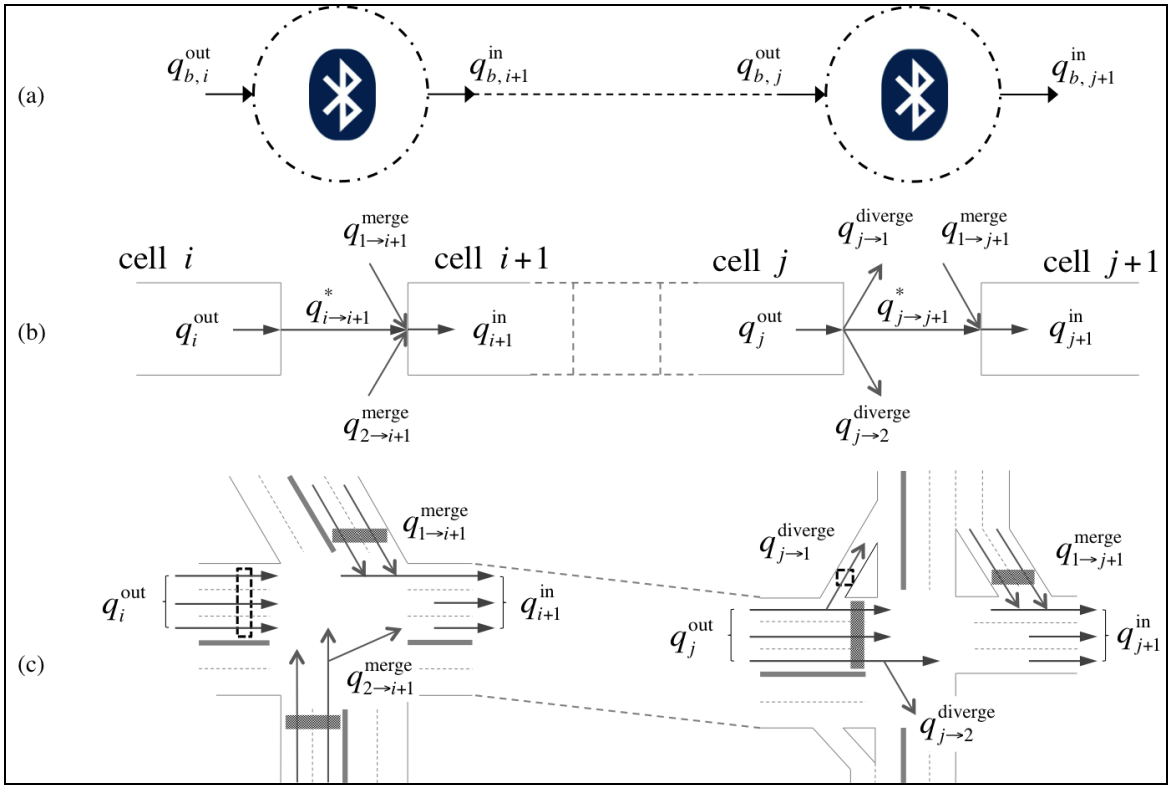

Figure 2. Example of CTM-based segmentation scheme at the intersections, and integration with Bluetooth data. (a) The real diameter of the Bluetooth scanning areas is assumed to be similar to the size of the intersections. (c) The dark-coloured boxes represent loop detectors. The dashed-lined boxes are an indication that some loop detectors may not be installed, or may temporarily fail.

In order to model the signalized intersections, the discrete model presented in the previous section is extended, by including merge and diverge nodes. To this end, the flow from, and into, the cells adjacent to each intersection is split into diverging, q^{diverge}, merging, q^{merge}, an in-between flow, q^{*} (Figure 2). These new flows are restricted by demand, supply, *turn fraction*, and *green-splits*. In particular, the in-between flow, for the generic class from cell $i-1$ to cell i, reads:

$$q^{*}_{u,i-1\to i} = \min\left(\alpha_{u,i-1\to i}\delta_{u,i-1}, \beta_{u,i-1\to i}\sigma_{u,i} \right) \tag{8}$$

with $\alpha_{u,i-1\to i}$ being the fraction of vehicles going through the intersection. The *reduction factor* $\beta_{u,x\to i}$, from the cell x to i, is computed as follows

$$\beta_{u,x\to i} = \varphi_{x\to i} \max\left(\gamma_{x\to i}, 1 - \sum_{y\neq x} \frac{\varphi_{y\to i}\alpha_{u,y\to i}\delta_{u,y}}{\sigma_{u,i}} \right) \tag{9}$$

where $\varphi_{x\to i}$ is the green-split for the approach x to i, and $\gamma_{x\to i}$ the priority of the approach x to i, over the other competing approaches. Eq. (8) is a more general version of the model in Tampère et al. (2011), for unsignalized intersections. In the case of a non-signalized intersection, the green split, φ, will be set to 1, for all incoming and diverging flows, and Eq. (9) reduces to the model in (Tampère, Corthout and Cattrysse 2011). Note that the green-split and priority ratios do not depend on the class, for signal and priority rules apply equally to all vehicles. Finally, the flows for the merging and

diverging cells are

$$\begin{cases} q^{\text{merge}}_{u,x\to i} = \min(\ \alpha_{u,x\to i}\delta_{u,x}, \beta_{u,x\to i}\sigma_u) \\ q^{\text{diverge}}_{u,i-1\to x} = \min(\ \alpha_{u,i-1\to x}\delta_{u,i-1}, \varphi_{i-1\to x}\sigma_{u,x}) \end{cases} ;\ \forall x \neq i \wedge\ x \neq i-1 \qquad (10)$$

For the above equations to be valid, it is important that both, the fraction, $\alpha_{u,i\to x}$, of the flows going from cell i to x, and the priorities, $\gamma_{x\to i}$, of the flows merging into cell i, all sum to one. To be sure, the total outgoing flow, for all vehicles of class u, from a cell i, upstream to an intersection is given by

$$q^{\text{out}}_{u,i} = \sum_{x\neq i+1} q^{\text{diverge}}_{u,i\to x} + q^{*}_{u,i\to i+1} \qquad (11)$$

that is, the sum of all lateral outflows plus the contribution from the in-between flow. Similarly, the total incoming flow from a cell, i, downstream to an intersection is

$$q^{\text{in}}_{u,i} = \sum_{x\neq i-1} q^{\text{merge}}_{u,x\to i} + q^{*}_{u,i-1\to i} \qquad (12)$$

These flows will need to be plugged into Eq. (2), in order to determine the density of the cells. It should be noted that Eq.(11) and (12) are general, in that they can be used to describe the flow between any pair of adjacent cells, within the target road. Indeed, it is easy to show that, for any two adjacent cells $i-1$ and i, that are not separated by an intersection, the following relations hold

$$\begin{cases} q^{\text{in}}_{u,i} = \sum_{x\neq i-1} q^{\text{merge}}_{u,x\to i} + q^{*}_{u,i-1\to i} = \min(\ \delta_{u,i-1}, \sigma_{u,i}) \\ q^{\text{out}}_{u,i} = \sum_{x\neq i} q^{\text{diverge}}_{u,i-1\to x} + q^{*}_{u,i-1\to i} = \min(\ \delta_{u,i-1}, \sigma_{u,i}) \end{cases} \qquad (13)$$

Hence, if no intersection is present between two adjacent cells we have $q^{\text{out}}_{u,i-1} = q^{\text{in}}_{u,i}$, as imposed by the Cell-Transmission Model.

3. SEQUENTIAL ESTIMATION OF TRAFFIC STATE

Typically, the state of a road network is only partially observed. That is, the flow, density and speed of each cell are not directly available. Instead, only limited information is available at the intersections. For instance, if an intersection has stop-line detectors installed in all lanes and on all approaches, one can measure the mixed-class flows at the intersections q^{diverge}, q^{merge}, and q^{*}. With the Bluetooth data available it becomes possible to estimate the average speed, $\bar{v}$, that the individual (Bluetooth) vehicles have maintained between any two scanned intersections, within some observation time. This speed, computed as the travel time-over-distance ratio, should be understood as the average of the speed values of the N consecutive cells, between the Bluetooth scanners located at the upstream of cells i and $i+N-1$, that is

$$\bar{v}_{i:i+N-1} = \frac{1}{N}\sum_{c=i}^{i+N-1} v_c \qquad (14)$$

The partial outflow, q^{out}_b, and inflow, q^{in}_b, can also be extracted from the Bluetooth recordings. These latter quantities are the flows of the Bluetooth class, from the cells adjacent to the scanned intersection (Figure 2). Note that all observations contain some level of uncertainty or noise. This noise is to attribute, among other factors, to the location of the stop-line detectors and the aggregation time used to collect the vehicle counts, the variable scanning area, and the finite scanning frequency of the

Bluetooth sensors. In this work, we shall assume that all uncertainties of the system are additive, Gaussian and zero-mean. Under this assumption, if we let $\mathbf{x}^{t+1}$ be the current state (vector) of the dynamical system, and $\mathbf{y}^{0,\dots t,t+1}$ the set of measurements available to date, about $\mathbf{x}^{0,\dots,t,t+1}$, the complete model of the system becomes

$$\begin{cases} \mathbf{x}^{t+1} = f(\mathbf{x}^t, \mathbf{u}^t) + \xi^t & \xi^t \propto \aleph(0, W^t) \\ \mathbf{y}^{t+1} = h(\mathbf{x}^{t+1}) + \vartheta^{t+1} & \vartheta^{t+1} \propto \aleph(0, R^{t+1}) \end{cases} \tag{15}$$

were $\mathbf{u}$ is an external input; and ξ and ϑ are independent Gaussian noise terms of zero-mean and covariance matrices W and R, respectively. The update function, f, encompasses all models presented earlier for the update of the state variables, such as density, k, and flow, q, for each cell. These are, Eq. (1) to (6) and (8) to (12). Other state variables, in $\mathbf{x}$, are also the fraction, λ, of vehicles belonging to the Bluetooth class. The state vector is mapped to the measurement vector, $\mathbf{y}$, through a function h, like the one given by Eq. (7) and (14). Therefore, the vector $\mathbf{x}$, for a stretch of C cells, can be written as

$$\mathbf{x}^t = (k_1^t, \dots, k_C^t, q_1^{\text{in},t}, \dots, q_C^{\text{in},t}, q_C^{\text{out},t}, \lambda_1^t, \dots, \lambda_C^t)^T \tag{16}$$

The input $\mathbf{u}$, includes the incoming demand, δ, upstream to the first cell; the supply, σ, downstream to the last cell; the lateral demand and supply of merging and diverging cells; and the green-splits, φ, at the intersections. Since these input demand and supply are usually not known, a *random walk* strategy can be used, as part of f, in order to update them. The input vector will also contain the lateral inflows, q^{merge}, and outflows, q^{diverge}, at the intersections. As for the demand and supply, the lateral flows can be partially or totally unobserved. In general, the system will need to maintain the *hidden* components of $\mathbf{u}$, in order for them to be estimated overtime.

The measurement vector, $\mathbf{y}$, contains the quantities that are observed, for instance, through the loop detectors and the BT scanners. A typical measurement vector, for a stretch of I intersection, is

$$\mathbf{y}^t = (q_\bullet^{\text{merge},t}, q_\bullet^{\text{diverge},t}, q_\bullet^{*,t}, q_{b,1}^{\text{in},t}, \dots, q_{b,I}^{\text{in},t}, q_{b,1}^{\text{out},t}, \dots, q_{b,I}^{\text{out},t}, \bar{v}_\bullet^t)^T \tag{17}$$

where we have denoted by $q_\bullet$, the flows available from the stop-line detectors. The symbol $\bar{v}_\bullet$ indicates the generic average speed value, computed from pairs of Bluetooth scanners, located along the target stretch. In this work, the parameters of our model are the free-flow speed v_f, jam density k_j, maximum flow q_m, and priority ratios, γ.

3.1 Particle Filter-Based Estimation

Bayes filters offer an elegant solution to the problem of estimating and predicting the *hidden* state of a system, from limited and noisy observations. To this end, a posterior $P(\mathbf{x}^{t+1} \mid \mathbf{y}^{0,\dots t,t+1})$, also known as *belief*, is maintained overtime, through a *sense* and *update* mechanism. The type of Bayes filter used in this work is the Particle Filter, which is a Sequential Montecarlo Method (Arulampalam, Maskell and Gordon 2002). The belief about the state of the system is represented by a set of M hypotheses or *particles*, $\mathbf{x}_{(j)}, j = 1 \dots M$, each of which has an associated *importance* weight $w_{(j)}, j = 1 \dots M$. The standard particle filter algorithm works as follows. First, new particles $\mathbf{x}_{(j)}^{t+1}$ are generated from the previously computed particles $\mathbf{x}_{(j)}^t$, by sampling from the distribution $P(\mathbf{x}^{t+1} \mid \mathbf{x}_{(j)}^t, \mathbf{u}^t)$, which is assumed to be known. The related weights are then updated as $w_{(j)}^{t+1} = P(\mathbf{y}^{t+1} \mid \mathbf{x}_{(j)}^{t+1})$. All weights are

normalized so that $\sum_j w_{(j)}^{t+1} = 1$. Finally, the belief $P(\mathbf{x}^{t+1} \mid \mathbf{y}^{0,\dots t,t+1})$ is expressed through M new particles, $\hat{\mathbf{x}}_{(j)}^{t+1}$, drawn from $\mathbf{x}_{(j)}^{t+1}$, with probability $w_{(j)}^{t+1}$. The *importance function* and *weight update* functions used in this work are

$$P(\mathbf{x}^{t+1} \mid \mathbf{x}_{(j)}^{t}, \mathbf{u}^{t}) = \aleph(\mathbf{x}^{t+1} \mid f(\mathbf{x}_{(j)}^{t}, \mathbf{u}^{t}), W^{t})$$
$$P(\mathbf{y}^{t+1} \mid \mathbf{x}_{(j)}^{t+1}) = \aleph(\mathbf{y}^{t+1} \mid h(\mathbf{x}_{(j)}^{t+1}), R^{t+1}) \qquad (18)$$

where $\aleph(\bullet)$ is the multivariate Normal distribution; the functions f and h, presented in the previous section, become the mean; W and R are the covariance matrices discussed earlier which, in this paper, are assumed constant and diagonal. The elements of the diagonal are the standard deviations that quantify system and measurement uncertainties.

4. APPLICATION TO REAL DATA

Our case study concerns a section of an arterial road (Coronation Drive) of the Brisbane metropolitan area, linking four signalized intersections. The three road segments, connecting the four intersections, have length 435m, 330m, and 710m. Each segment was partitioned into a number of cells, such that the cell lengths were always longer than the free-flow travel distance, that is, $\Delta x \geq v_f \Delta t_{\text{sim}}$. This ensured the stability of the Cell-Transmission Model, and its convergence to the analytical solution. The resulting total number of cells was 7. The simulation step, Δt_{sim}, was 10 seconds. The observation time step, Δt_{obs}, for the loop detectors was 5 minutes, whereas the average speed from the Bluetooth vehicles was available at irregular time intervals. Before running the simulation, these data was then aggregated into 5 minute-time bins, and the average for each bin was computed. Because the simulation time step was a sub-multiple of the simulation time step, $\Delta t_{\text{obs}} = n\Delta t_{\text{sim}}$, the weights, $w_{(j)}$, of the particle filter were updated once every n re-samplings (30 in our experiments) of the particles $\mathbf{x}_{(j)}$; then, a new set of particles $\hat{\mathbf{x}}_{(j)}$ was drawn, with probability specified by the updated weights. A total of 300 particles was used for the estimation. Flow and density of each cell, i, were assumed to be related by a triangular fundamental function, $Q_i(k_i)$, like the one depicted in Figure 1. The system parameters were kept constant at reasonable values. In particular, the free-flow speed, v_f, was set to the speed limit of 16.67 mps (meters-per-second), the saturation flow, q_m, was set to n_l 1.5278 vps (vehicles-per-second), where n_l is the number of lanes (3 in our case) and 1.5278 is the number of personal cars per second, common for arterial roads. The jam density, k_j, was set to n_l 0.1333 vpm (vehicles-per-meter), with 0.1333 being the maximum number of cars that can be found within one meter of arterial stretch. Finally, the priority ratios, γ, were given a value of 0.8 for the target stretch, and 0.2 for the rest of the approaches, to indicate that the target line has always higher priority over the incoming flows from the merging roads. The standard deviation values of the model and the parameters of the system are reported in Table 1. In our experiments, the flow data from the stop-line detectors was only available for the three, out of four, downstream intersections. The green-splits, φ, were available for all approaches. The Bluetooth-based average speed used, as part of the measurement vector, was that recorded between the first and third intersection (cells 1 to 3), $\bar{v}_{1:3}$, and between second and fourth intersection, $\bar{v}_{2:7}$, (cells 2 to 7). The other three speed measurements $\bar{v}_{1:2}$, $\bar{v}_{2:2}$ and $\bar{v}_{3:7}$ available were left out, for qualitative comparisons between the speed predicted by the model, and that measured through the Bluetooth scanners. The results in Figure 3 are based on the

simulation from the dataset, as of Wednesday 3 October 2012.

Preliminary results show that our system is capable of recovering the hidden spatio-temporal evolution of density, flow, speed and Bluetooth Penetration Rates (Figure 3, right); as well as the demand and supply of the merging and diverging cells. Moreover, the model can reproduce the capacity-drop phenomenon observed in arterial roads (Wu, Liu and Geroliminis 2011), due to the green-split and the sub-optimal coordination from the fixed turning volumes at the intersections (Figure 3c). The mechanism proposed offers robust filtering and predictive capabilities, in that the actual state of the system can be estimated and predicted, even in the presence of significant measurement noise (Figure 3a). Finally, including the fraction of Bluetooth vehicles into the model allows visualizing how the Bluetooth class moves within the target stretch, and how this affects the behaviour of the mixed class (Figure 3, right).

5. CONCLUDING REMARKS

This paper has formulated a new model-based framework for the state estimation of traffic flow using emerging BT data. We have applied a Bayes filter to derive the posterior of the estimated state, from the loop detector and BT data available. The filter implements a Sequential Montecarlo Method, which incorporates a two-class Cell-Transmission Model (CTM). The two classes are the BT-equipped vehicles and the mixed-class. The data used concerned a section of an arterial road (Coronation Drive) of the Brisbane metropolitan area, linking four signalized intersections. Numerical results have indicated the potentials of using partial BT data in reconstructing the real-time traffic states. Part of our future research, will be dedicated to the validation of the estimated flow and speed values with network corridors. Indeed, although we have shown how the Bluetooth data can be factored into the CTM in order to enhance the estimation of the traffic state, the experiments presented are not meant to establish the validity of our approach. A rigorous validation can be achieved by considering other reliable sources of data, such as GPS data.

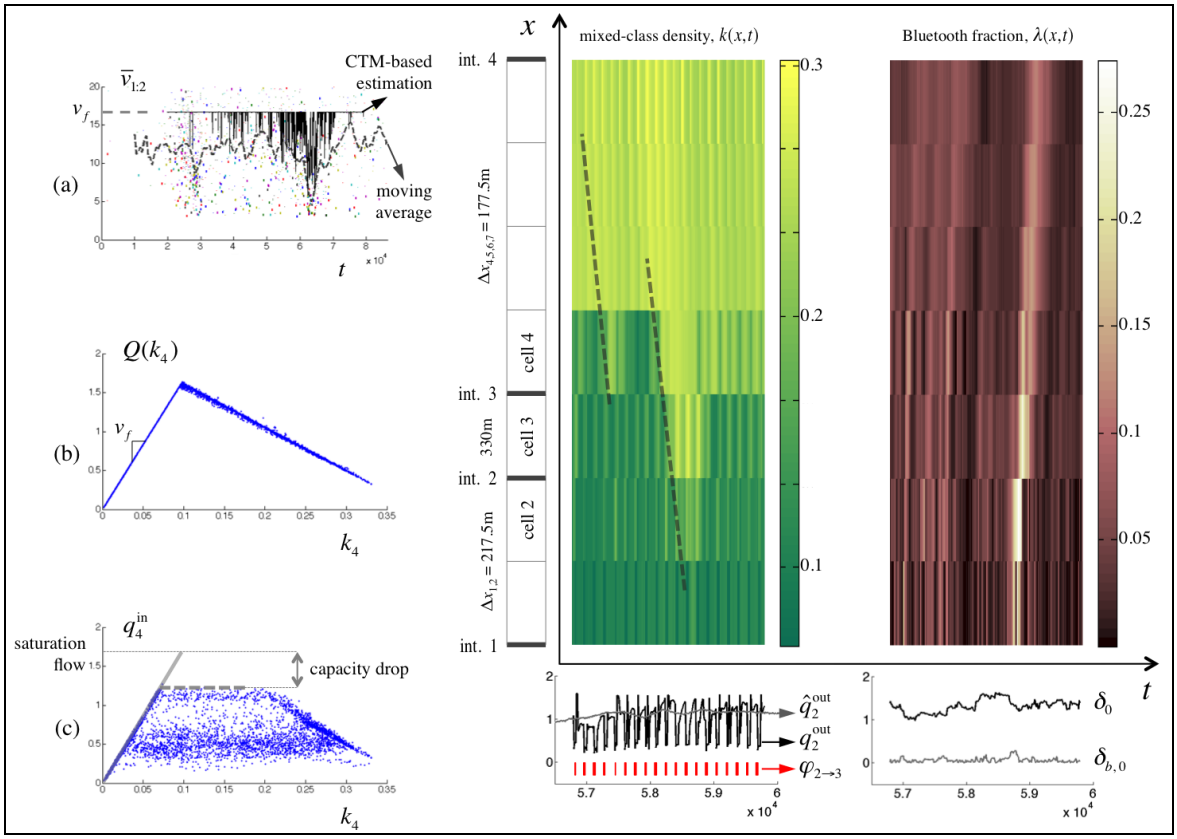

Figure 3. (centre) Cell segmentation of the target arterial road. Darker, horizontal bars indicate the location of the 4 intersections, at which the LD and BT data was collected. (right) The CTM-based filter can predict the formation of shock waves (highlighted by diagonal dashed lines). Flow fluctuations, triggered by green-splits φ, are predicted upstream to the intersections. Note how the predicted flow, q, follows the observation $\hat{q}$ (5 minute aggregations of vehicle counts); and how the upstream demand, δ_0, is estimated for both classes. (a) The moving average (dashed line), computed on the noisy dataset (dots), appears to diverge from the speed estimated by CTM-based filter. The estimation is consistent with all observations. (b) Cell-wise density-flow plot. (c) Capacity drop, observed from the estimated flow and density, downstream to the third intersection.

Table 1. Parameters of the model

system parameters				density	flow	BTPR	demand & supply	obs. flow	obs. speed
v_f [mps]	q_m [vps]	k_j [vpm]	$\gamma_{i-1\to i}$	W_k	W_q	W_λ	W_{ds}	R_q	$R_{\bar{v}}$
16.67	1.58	0.4	0.8	$1\cdot10^{-6}$	$1\cdot10^{-5}$	$1\cdot10^{-5}$	$1\cdot10^{-3}$	$1\cdot10^{-4}$	$1\cdot10^{-1}$

REFERENCES

Arulampalam, M. S., S. Maskell and N. Gordon. (2002) A tutorial on particle filters for online nonlinear/non-Gaussian Bayesian tracking. *IEEE Transactions on Signal Processing* 50 (2): pp. 174-188.

Bachmann, C., M. J. Roorda, B. Abdulhai and B. Moshiri. (2013) Fusing a Bluetooth Traffic Monitoring System With Loop Detector Data for Improved Freeway Traffic Speed Estimation. *Journal of Intelligent Transportation Systems: Technology, Planning and Operations* 17 (2), pp. 152-164.

Daganzo, C. F. . (1994) The cell transmission model: A dynamic representation of highway traffic consistent with the hydrodynamic theory. *Transportation Research Part B* 28 (4), pp. 269-287.

Daganzo, C. F. . (1995) The cell transmission model, part II: Network traffic. *Transportation Research Part B* 29 (2), pp. 79-93.

Lighthill, M. J. and G. B. Whitham. (1955) On Kinematic Waves. II. A Theory of Traffic Flow on Long Crowded Roads. *Proc. R.oy Soc. Lond. A* 229 (1178), pp. 317--345.

Mehran, B. and M. Kuwahara. (2013) Fusion of probe and fixed sensor data for short-term traffic prediction in urban signalized arterials. *International Journal of Urban Sciences* 17 (2), pp. 163-183.

Mihaylova, L., R. Boel and A. Hegyi. (2007) Freeway traffic estimation within particle filtering framework. *Automatica* 3 (2), pp. 290--300.

Richards, P. I. (1956) Shock Waves on the Highway. *Operations Research* 4 (1), pp. 42--51.

Tampère, C. M. J., R. Corthout and L. H. Immers Cattrysse. (2011) A generic class of first order node models for dynamic macroscopic simulation of traffic flows. *Transportation Research Part B* 45 (1), pp. 289--309.

Work, D.B. , O.-P. Tossavainen, Q. Jacobson and A.M. Bayen. (2009) Lagrangian sensing: traffic estimation with mobile devices. In *American Control Conference 2009. ACC '09., St. Louis, Missouri, USA*, edited.

Wu, X., H. X. Liu and N. Geroliminis. (2011) An empirical analysis on the arterial fundamental diagram. *Transportation Research Part B* 45 (1), pp. 255 - 266.

Y., Yufei, J. W. C. van Lint, R. E. Wilson, F. van Wageningen-Kessels and S.P. Hoogendoorn. (2012) Real-Time Lagrangian Traffic State Estimator for Freeways. *IEEE Transactions on Intelligent Transportation Systems* 13 (1), pp. 59--70.